Proc. Natl. Acad. Sci. USA
Vol. 93, pp. 3362–3367, April 1996
Neurobiology

N-Methyl-D-aspartate receptor-induced proteolytic conversion of postsynaptic class C L-type calcium channels in hippocampal neurons

JOHANNES W. HELL*†, RUTH E. WESTENBROEK*, LIAM J. BREEZE*, KEVIN K. W. WANG‡, CHARLES CHAVKIN*, AND WILLIAM A. CATTERALL*

*Department of Pharmacology, Mailbox 357280, University of Washington, Seattle, WA 98195-7280; and ‡Parke–Davis Pharmaceutical Research Division, Warner–Lambert Co., Ann Arbor, MI 48105-2430

Contributed by William A. Catterall, December 26, 1995

ABSTRACT **Ca^{2+} influx controls multiple neuronal functions including neurotransmitter release, protein phosphorylation, gene expression, and synaptic plasticity. Brain L-type Ca^{2+} channels, which contain either α_{1C} or α_{1D} as their pore-forming subunits, are an important source of calcium entry into neurons. α_{1C} exists in long and short forms, which are differentially phosphorylated, and C-terminal truncation of α_{1C} increases its activity ≈4-fold in heterologous expression systems. Although most L-type calcium channels in brain are localized in the cell body and proximal dendrites, α_{1C} subunits in the hippocampus are also present in clusters along the dendrites of neurons. Examination by electron microscopy shows that these clusters of α_{1C} are localized in the postsynaptic membrane of excitatory synapses, which are known to contain glutamate receptors. Activation of *N*-methyl-D-asparatate (NMDA)-specific glutamate receptors induced the conversion of the long form of α_{1C} into the short form by proteolytic removal of the C terminus. Other classes of Ca^{2+} channel α_1 subunits were unaffected. This proteolytic processing reaction required extracellular calcium and was blocked by inhibitors of the calcium-activated protease calpain, indicating that calcium entry through NMDA receptors activated proteolysis of α_{1C} by calpain. Purified calpain catalyzed conversion of the long form of immunopurified α_{1C} to the short form *in vitro*, consistent with the hypothesis that calpain is responsible for processing of α_{1C} in hippocampal neurons. Our results suggest that NMDA receptor-induced processing of the postsynaptic class C L-type Ca^{2+} channel may persistently increase Ca^{2+} influx following intense synaptic activity and may influence Ca^{2+}-dependent processes such as protein phosphorylation, synaptic plasticity, and gene expression.**

A variety of neuronal functions such as neurotransmitter release, protein phosphorylation, gene expression, and synaptic plasticity are regulated by voltage-gated Ca^{2+} channels (1–4). Five types of Ca^{2+} channels can be distinguished based on pharmacological and physiological criteria: T-type channels are activated by small depolarizations, whereas high-threshold Ca^{2+} channel types L, N, P, and Q require strong depolarization to open (5, 6). Brain Ca^{2+} channels are composed of a pore-forming α_1 subunit in association with $\alpha_2\delta$ and β subunits (7). Five different classes of α_1 subunits (classes A–E) encoding high-threshold Ca^{2+} channels have been cloned and sequenced from mammalian brain cDNA (5, 8). Classes C and D are the two major L-type channels present in the mammalian brain (9–11) and constitute an important route of Ca^{2+} entry into neurons (12, 13). In most areas of the brain, L-type channels are localized in cell bodies and proximal dendrites (14, 15), but in the CA3 region of the hippocampus α_{1C} is also present along the full length of dendrites (11). Although α_{1D} is smoothly distributed over the surface of cell bodies and proximal dendrites, α_{1C} is clustered (11) in a pattern that is typical for synaptic proteins.

Similar to the α_1 subunit of the skeletal muscle L-type channel (α_{1S}; refs. 16–19), α_{1C} exists in two size forms with apparent molecular masses in the range of 180–190 and 210–220 kDa (11, 20), the short form of α_{1C} is truncated at the C terminus (20), and the two size forms of α_{1C} are differentially phosphorylated by cAMP-dependent protein kinase *in vitro* as well as in intact hippocampal neurons (20, 21). Elimination of the last 307–472 amino acids from the C terminus of α_{1C} by truncation of the cDNA gives rise to a Ca^{2+} channel with 4- to 6-fold higher ion conductance activity than the full-length form when expressed in *Xenopus* oocytes (22, 23). These findings suggest that the C terminus of α_{1C} exerts inhibitory control over the activity of class C L-type channels. Truncation of α_{1C} by a receptor-mediated pathway might result in sustained changes in the activity of class C L-type calcium channels.

Glutamate is the predominant excitatory neurotransmitter in the nervous system due to its activation of ionotropic receptors at postsynaptic sites (24). Glutamate receptors can be divided into three major classes by their sensitivity to the synthetic agonists AMPA, kainate, and *N*-methyl-D-aspartate (NMDA) (24). NMDA receptors are usually calcium permeable, while AMPA and kainate receptors in neurons usually are not (24). In these experiments, we show that activation of NMDA receptors in hippocampal neurons induces proteolytic truncation of the α_{1C} subunits of class C calcium channels located in the postsynaptic membrane through a pathway involving calcium influx and activation of the calcium-regulated protease calpain (25). This pathway may result in sustained changes in the activity of L-type calcium channels in the postsynaptic membrane.

EXPERIMENTAL PROCEDURES

Materials. The ECL detection kit for immunoblotting was obtained from Amersham; protein A-Sepharose and bovine serum albumin (IgG-free) were from Sigma; tetrodotoxin and calpain inhibitors I and II were from Calbiochem; and NMDA, (+)-MK801, *R*(−)-3-(2-carboxypiperazin-4-yl)-propyl-1-phosphonic acid (CPP), and (±)2-amino-5-phosphonopentanoic acid (AP5) were from Research Biochemicals (Natick, MA). Calpain I and II were purified by established procedures (26, 27). Three-week-old and adult Sprague–Dawley rats were

The publication costs of this article were defrayed in part by page charge payment. This article must therefore be hereby marked "*advertisement*" in accordance with 18 U.S.C. §1734 solely to indicate this fact.

Abbreviations: AP5, 2-amino-5-phosphonopentanoic acid; CPP, *R*(−)-3-(2-carboxypiperazin-4-yl)-propyl-1-phosphonic acid; NMDA, *N*-methyl-D-aspartate.

†Present address: Department of Pharmacology, University of Wisconsin, Madison, WI 53706-1532.

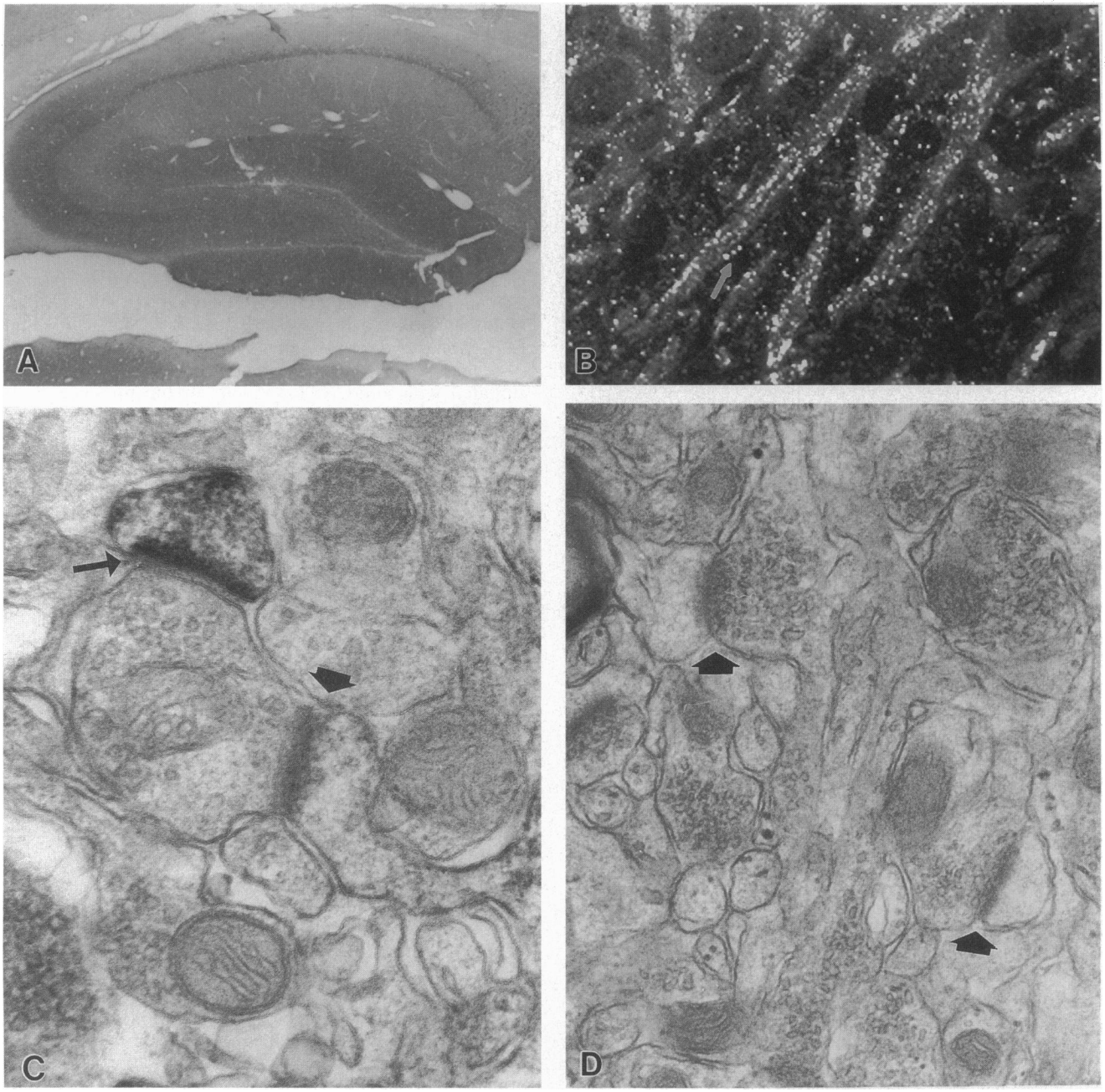

FIG. 1. Localization of class C L-type channels at postsynaptic densities of dendritic spines. (*A*) Anti-CNC1 staining of the hippocampus at the light microscopic level. (×15.) (*B*) A confocal image at higher magnification illustrating the staining (in white) of punctate structures with the appearance of spine heads (arrow) along the proximal dendrites of CA3 pyramidal neurons. (×290.) (*C*) Electron micrograph of the dendritic field of the hippocampal CA3 region illustrating a CNC1 positive (thin arrow) and a nonimmunoreactive (broad arrow) postsynaptic density associated with asymmetric synaptic contacts. (×70,400.) (*D*) Control section in which no primary antibody was used. Broad arrows point to unlabeled asymmetric synaptic contacts. (×38,200.)

obtained from Bantin & Kingman (Bellevue, WA). Production, preparation, and characterization of the anti-peptide antibodies anti-CNB1, -CNC1, -CNC2, and -CNE2 against α_{1B}, α_{1C}, and α_{1E}, respectively, have been described (20, 28–30).

Immunocytochemistry. Adult rats were anesthetized with sodium pentabarbitol and perfused with 4% paraformaldehyde and 0.25% glutaraldehyde in 0.1 M sodium phosphate buffer. Brains were removed, postfixed for 2 h, and sunk in 10% and 30% sucrose. Tissue for light microscopy was processed as described (11). For electron microscopy, 80 μm coronal sections were cut on a sliding microtome, rinsed in 100 mM Tris·HCl (pH 7.4) (TB; 10 min) followed by 0.5% H_2O_2 (30 min), 1.0% H_2O_2 (60 min), and 0.5% H_2O_2 in TB (30 min), TB (15 min), and 150 mM NaCl in 10 mM Tris·HCl (pH 7.4) (TBS; 15 min), blocked in TBS containing 3% normal goat serum, 3% bovine serum albumin, and 0.4% dimethyl sulfoxide (blocking solution; 60 min), and incubated with affinity-purified anti-CNC1 antibody (10–20 μg/ml) overnight at room temperature. The primary antibody was visualized and the samples were processed for electron microscopy as described (31). All antibodies were diluted with blocking solution. Controls included replacing anti-CNC1 antibody with no serum or preabsorbing anti-CNC1 antibody for 8 h with 25 μM CNC1 peptide.

Preparation and Treatment of Hippocampal Slices. Hippocampal slices were prepared from rat brain and incubated for biochemical experiments as described (21). For recording of population spikes, slices were kept in a perfusion chamber

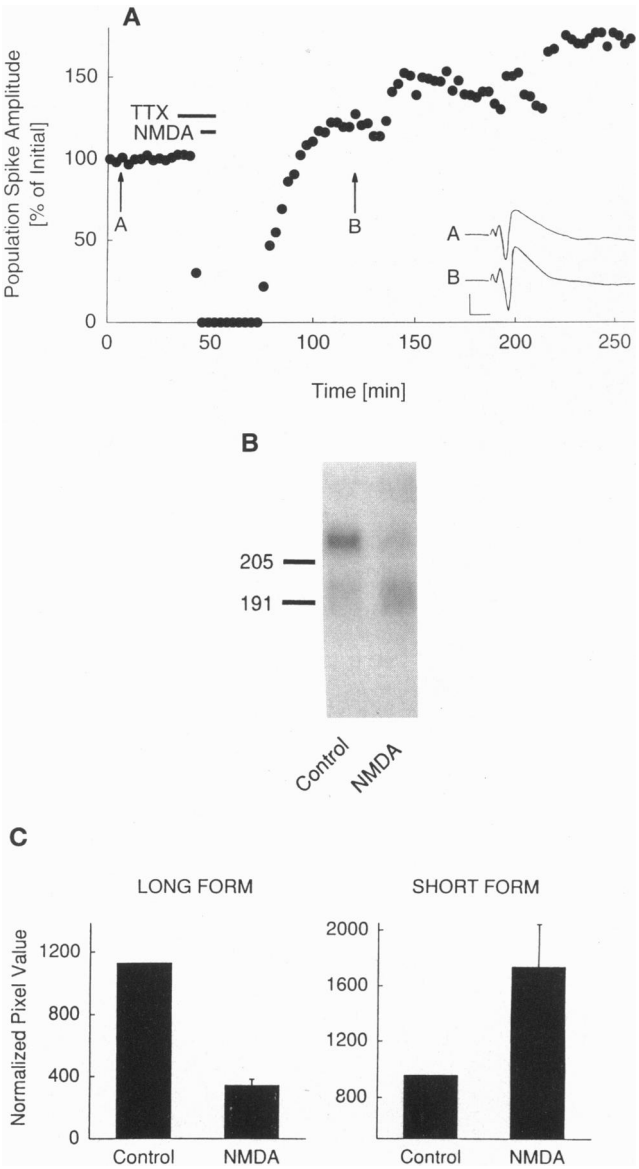

FIG. 2. Enhanced synaptic transmission and conversion of α_{1C} to its short form during treatment with NMDA. (*A*) Population spikes of hippocampal pyramidal neurons in CA1 elicited by stimulation of the Schaffer collaterals before and after bath application of 200 μM NMDA for 5 min when 1 μM tetrodotoxin was present as indicated (bars). Slices were pretreated with 1 μM tetrodotoxin for 25 min and incubated with or without NMDA (200 μM). Drugs were removed from the incubation buffer after 5 min. (*Inset*) Population spikes measured before (A) and after (B; see arrows) NMDA treatment, demonstrating potentiation of the population spikes by NMDA application. Size of the population spike continued to increase over the next 2 h. Bars: 1 mV (vertical) and 5 ms (horizontal). Similar results were obtained in two other experiments. (*B*) Effect of NMDA treatment on molecular mass of α_{1C}. For biochemical analysis, slices were incubated with 1 μM tetrodotoxin for 25 min and then with 200 mM NMDA and tetrodotoxin for 5 min. Both drugs were washed out, slices were incubated for another 60 min, and Ca^{2+} channels were immunoisolated by immunoprecipitation with anti-CNC1, analyzed by SDS/PAGE, and immunoblotted as described (28). Protein markers of 191 and 205 kDa are indicated at the left. (*C*) Quantitative analysis of conversion of the long form of α_{1C} into the short form in the presence of NMDA. Immunoblotting signals of the long and short forms of α_{1C} were quantified for 10 experiments by densitometry. To normalize the data, the average of the pixel values of the long form and the average of the short form as obtained from all control incubations were calculated (shown as Control) and the values for the NMDA incubations were calculated relative to control for each experiment and averaged (shown as NMDA ± SEM). Note that the amount of decrease of the long form approximately equals the amount of increase of the short form.

and recordings were made as described (32). For both biochemical and electrophysiological experiments, drugs were applied after a 90-min equilibration at 32°C in the perfusion chamber.

Calpain Treatment of Immunopurified α_{1C}. Full-length α_{1C} was immunoprecipitated from digitonin-solubilized rat brain membranes with the C-terminal-specific antibody anti-CNC2 as described (20). The anti-CNC2 precipitates were rinsed with 1 ml of 10 mM dithiothreitol/25 mM Tris·HCl, pH 7.4/1 μM pepstatin A/200 μM phenylmethanesulfonyl fluoride/1 mM 1,10-phenanthroline and incubated in 100 μl of this buffer supplemented with 5 mM Ca^{2+} (control medium), 0.5 mM Ca^{2+} plus 25 ng of calpain I, or 5 mM Ca^{2+} plus 100 ng of calpain II for 2 min at room temperature before calpain inhibitor I and II (20 μM each), 20 mM EDTA, and 10 mM EGTA were added on ice to stop the reaction. Protein A-Sepharose was removed by centrifugation. α_{1C} was reprecipitated with anti-CNC1 antibody in the presence of 1% Triton X-100 and immunoblotted with anti-CNC1 antibody as described (20).

RESULTS AND DISCUSSION

Postsynaptic Localization of Class C L-Type Channels in the Hippocampus. In the hippocampus, the α_{1C}-specific antibody anti-CNC1 (11) showed immunoreactivity throughout the dendritic fields of the CA2 and CA3 area and the dentate gyrus (Fig. 1*A*). In the CA1 area, anti-CNC1 staining was concentrated in neuronal cell bodies as in most other regions of the brain, but a clearly detectable level of immunostaining was also observed in the dendritic field of the CA1 pyramidal neurons (Fig. 1*A*). Confocal imaging exhibited a clustered distribution of the anti-CNC1 immunoreactivity along dendrites of pyramidal neurons in the hippocampus (Fig. 1*B*), as previously observed with peroxidase-antiperoxidase staining (11). Electron microscopy revealed that these clusters of immunoreactivity are localized primarily at postsynaptic densities of asymmetric synapses (Fig. 1*C*). These synapses are localized on dendritic spines (Fig. 1*C*) as well as on dendritic shafts and cell bodies (not shown). This finding suggests that class C L-type calcium channels are colocalized with NMDA receptors and other glutamate receptors, which are clustered in the postsynaptic membrane at excitatory synapses (24, 33). Some spines were found to lack α_{1C} immunoreactivity and therefore served as internal negative controls when seen next to immunoreactive spines (Fig. 1*C*). Additional negative controls included incubations with anti-CNC1 in the presence of the CNC1 peptide (not shown) and incubation without the primary antibody (Fig. 1*D*). No significant staining of postsynaptic densities was observed in the control samples. Recent Ca^{2+} imaging studies also suggest the presence of voltage-activated Ca^{2+} channels in dendritic spines (34, 35), complementing our results.

Effect of NMDA Treatment on Synaptic Transmission at the Schaffer Collateral/CA1 Synapse. The presence of class C L-type calcium channels in the postsynaptic membrane suggested that synaptic activation might induce posttranslational modifications of α_{1C} by protein phosphorylation or by receptor-activated proteolytic processing. To examine this possibility, we developed conditions under which NMDA receptors could be activated by bath-applied NMDA without damage to pyramidal neurons in hippocampal slices maintained under physiological conditions *in vitro* as described (32). NMDA (200 μM) was applied for 5 min in the presence of 1.3 mM $MgCl_2$ and the Na^+ channel blocker tetrodotoxin in order to prevent electrical excitation and release of neurotransmitters in re-

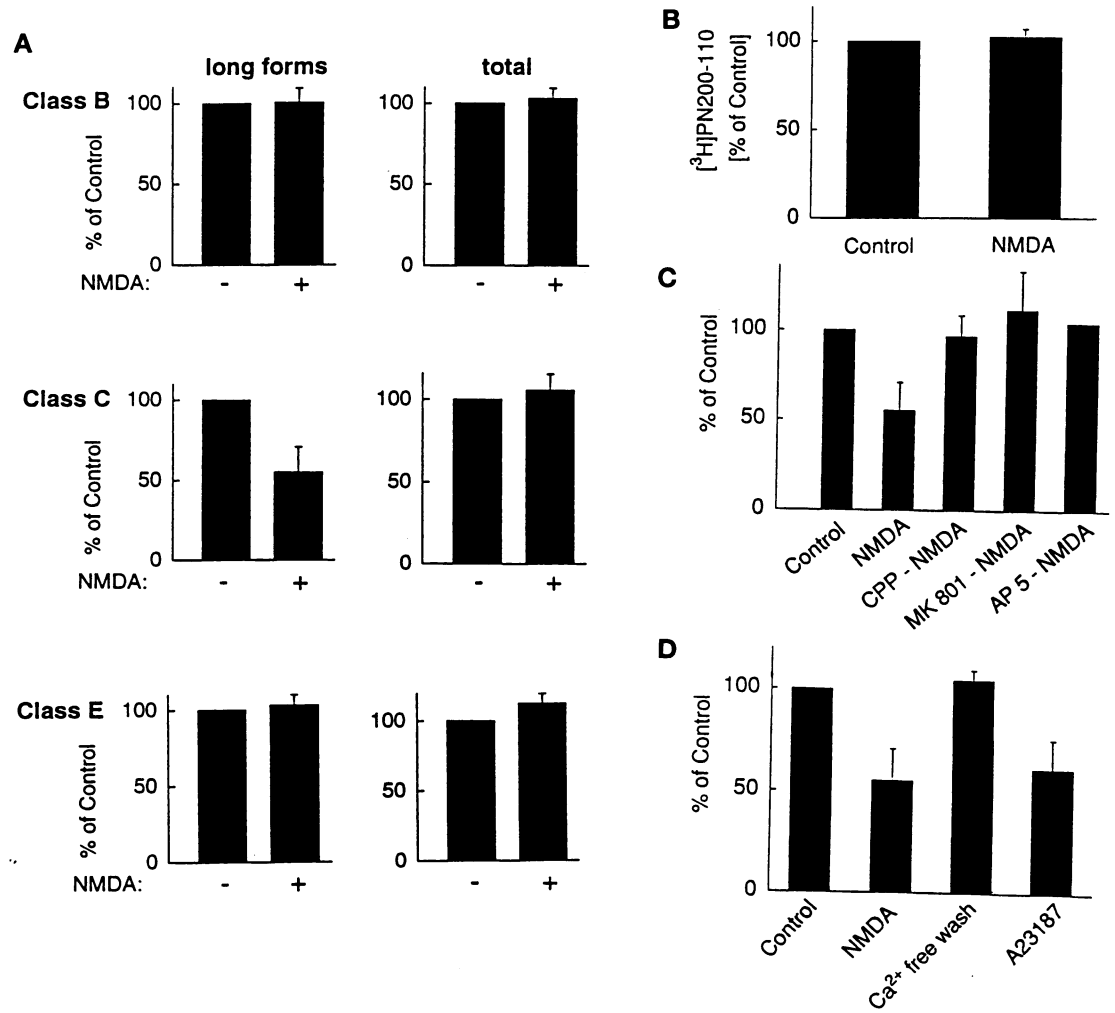

FIG. 3. NMDA-induced proteolytic conversion of α_{1C} into its short form. (*A*) Hippocampal slices were treated with NMDA in the presence of tetrodotoxin as described in Fig. 2. The α_{1B}, α_{1C}, and α_{1E} subunits of brain calcium channels were immunoprecipitated with specific antibodies, resolved by SDS/PAGE, and visualized by immunoblotting as described (21). The amount of the long and short forms of each α_1 subunit was determined by densitometric scanning. The NMDA-induced conversion of the α_1-subunit long form into its short form as reflected by a decrease of the long form without any loss of total amount is observed for α_{1C} but not for α_{1B} or α_{1E}. (*B*) Effect of NMDA on dihydropyridine binding to α_{1C}. Class C calcium channels were solubilized with digitonin (28) from hippocampal slices treated under control conditions or with NMDA as in *A*. Class C channels were isolated by immunoprecipitation with anti-CNC1, and specific binding of [^{3}H]PN200-110 was determined as described (21). (*C*) Effect of NMDA receptor blockers on NMDA-induced conversion of α_{1C} to its short form. α_{1C} was isolated from control and NMDA-treated hippocampal slices and analyzed by SDS/PAGE as in *A*. CPP (50 μM; $n = 3$), MK 801 (50 μM; $n = 3$), or AP5 (100 μM) was added as indicated 15 min before NMDA from 200-fold concentrated, neutralized stock solutions made in H_2O. (*D*) Effect of Ca^{2+} on NMDA-induced conversion of α_{1C} to its short form. α_{1C} was isolated from control and NMDA-treated hippocampal slices and analyzed by SDS/PAGE as in *A*. Ca^{2+} was removed immediately before NMDA addition by two washes of the slices with Ca^{2+}-free incubation buffer (Ca^{2+}-free wash). Ionophore A23187 (10 μM) was added to Ca^{2+}-containing buffer where indicated (A23187). All results are given as average ± SEM ($n = 3$–5) of relative amounts of the long form of α_{1C} in comparison to control treatments, which correspond to 100%.

sponse to NMDA-induced depolarization. This treatment should limit the effect of NMDA to postsynaptic sites containing NMDA receptors. Under these conditions, population spikes in response to stimulation of the Schaffer collaterals were inhibited during drug treatment but recovered completely after washing out both drugs (Fig. 2*A*), demonstrating that hippocampal neurons did not lose their functional integrity during NMDA treatment. Moreover, the population spike amplitude was increased by 10–30% after recovery of the slices from drug treatment and increased further over 2–3 h to 145% ± 21% of control ($n = 3$; $P < 0.05$), indicating that long-term potentiation of synaptic transmission had been induced by the NMDA treatment (see also ref. 36).

NMDA-Induced Proteolytic Processing of α_{1C}. The activity of class C L-type channels may be regulated by posttranslational modifications such as phosphorylation and proteolytic processing of its C terminus (20–23, 37). Since class C L-type Ca^{2+} channels are colocalized with NMDA receptors in the postsynaptic membrane, we tested the possibility that activation of NMDA receptors causes a structural modification of α_{1C}. Previous results indicated that the short form of α_{1C} in brain is truncated at the C-terminal end (20). A 5-min treatment of hippocampal slices with 200 μM NMDA causes a reduction in the amount of the long form and an increase in the amount of the short form as detected by immunoblotting with anti-CNC1, which recognizes both forms (Fig. 2*B*). Quantitative analysis revealed that the amount of long form lost after NMDA treatment approximately equaled the increase of short form (Fig. 2*C*), indicating that the proteolytic processing resulted in a defined modification rather than in extensive degradation of α_{1C}. Incubation with 50 or 200 μM NMDA decreased the long form by 40.7% ± 9.8% ($n = 5$) and 53.6% ± 16.4% ($n = 12$), respectively. In a series of experiments where the long form was decreased on average by 50%,

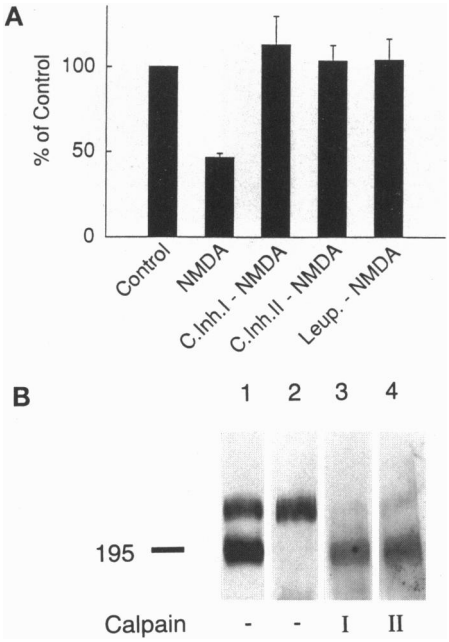

FIG. 4. Role of calpain in NMDA-induced processing of α_{1C}. (*A*) Hippocampal slices were stimulated with NMDA in the presence of tetrodotoxin as described in Fig. 2. α_{1C} was immunoprecipitated with specific antibodies, resolved by SDS/PAGE, and visualized by immunoblotting as described (28). Dimethyl sulfoxide (2 μl) containing no drugs (Control and NMDA) or 100 mM calpain inhibitor I (C.Inh.I), calpain inhibitor II (C.Inh.II), or leupeptin (Leup.) was added to slices in 1 ml of incubation buffer 15 min before NMDA was applied. Results are given as average ± SEM (n = 3–5) of relative amounts of the long form of α_{1C} in comparison to control treatments, which correspond to 100%. (*B*) Cleavage of the long form of α_{1C} by purified calpain I and calpain II. Lane 1, anti-CNC1 was used to immunoprecipitate both size forms of α_{1C}. The anti-CNC1 precipitate, which served as a control to indicate the migration positions of the long and short form of α_{1C}, was not further treated before SDS/PAGE and immunoblotting. Lanes 2–4, anti-CNC2, which is directed against the C terminus of the full-length form of α_{1C} (20), was used to specifically immunoprecipitate the long form of α_{1C}. The anti-CNC2 precipitates were incubated with control medium (lane 2), calpain I (lane 3), or calpain II (lane 4) and analyzed by SDS/PAGE and immunoblotting (20, 28).

the total amount of long and short form did not show any reduction (Fig. 3*A*). In addition, dihydropyridine binding to class C channels as detected after immunoprecipitation with anti-CNC1 was not reduced by NMDA treatment (Fig. 3*B*). Class B N-type and class E Ca^{2+} channels also exist in two different size forms, which differ at their C-terminal ends and are localized along dendritic shafts and at presynaptic sites (class B) or in neuronal cell bodies (class E) in the hippocampus (21, 28–30, 38, 39). Neither α_{1B} nor α_{1E} subunits are proteolytically processed after NMDA treatment (Fig. 3*A*), showing that NMDA-induced processing of Ca^{2+} channels is specific for α_{1C}. Inhibitor studies confirmed that induction of proteolytic processing of α_{1C} by NMDA was mediated by activation of NMDA receptors. The competitive antagonists AP5 and CPP (40) and the ion channel blocker MK-801 (40) all blocked the effect completely (Fig. 3*C*).

Calcium Dependence of NMDA-Induced Processing of α_{1C}. Activation of NMDA receptors increases calcium influx into neurons (41, 42). No processing of α_{1C} was detectable after removal of extracellular Ca^{2+}, suggesting that proteolytic processing is induced by Ca^{2+} influx through NMDA receptors (Fig. 3*D*). In agreement with this conclusion, processing of α_{1C} could also be evoked by application of the Ca^{2+} ionophore A23187 (10 μM) when extracellular Ca^{2+} was present (Fig. 3*D*). These results suggest that calcium influx through the NMDA receptor can induce the proteolytic processing of postsynaptic class C L-type calcium channels.

Proteolytic Processing of α_{1C} by Calpain. The Ca^{2+} dependence of proteolytic processing suggests that the Ca^{2+}-dependent cytosolic protease calpain (25), which is present in dendritic spines (43) and is activated by NMDA (44), may be responsible for the processing of α_{1C}. Three different calpain inhibitors (25) completely prevented the NMDA-induced processing of α_{1C} in hippocampal neurons (Fig. 4*A*), consistent with the hypothesis that calpain is responsible for processing of α_{1C}. To examine whether purified calpain could specifically cleave the long form of α_{1C} to the short form, we immunopurified class C calcium channels containing the long form of α_{1C} using anti-CNC2, an anti-peptide antibody that is directed against the amino acid sequence at the C terminus of α_{1C} and specifically precipitates the long form (20). Incubation of immunopurified class C calcium channels with purified calpain I or II catalyzed conversion of the long form of the α_{1C} subunits into the short form without extensive further proteolytic degradation (Fig. 4*B*). These results show that calpain is capable of proteolytic conversion of full-length α_{1C} to the short form *in vitro* and therefore provide further support for the hypothesis that calpain is responsible for the receptor-induced proteolytic conversion observed in hippocampal neurons.

Possible Physiological Significance of NMDA Receptor-Induced Proteolytic Processing of α_{1C}. Our results show that activation of NMDA receptors induces a permanent covalent modification of α_{1C} through Ca^{2+}-dependent activation of calpain. Cleavage of the C-terminal domain by calpain removes 250–300 amino acid residues, as estimated by the change in apparent molecular mass. Previous studies show that removal of 300–470 amino acid residues from the C terminus of α_{1C} by proteolytic enzyme treatment or by expression of cDNAs encoding truncated forms results in enhanced activation of Ca^{2+} channels in response to depolarization (22, 23). Therefore, it is likely that strong synaptic activation of NMDA receptors causes a persistent enhancement in voltage-dependent activation of class C L-type Ca^{2+} channels in postsynaptic membranes via this pathway. Increased activation of L-type Ca^{2+} channels in postsynaptic sites may amplify calcium transients resulting from synaptic activity and may participate in the calcium-dependent regulation of protein phosphorylation, gene transcription, and other events that are initiated in cell bodies and dendrites by synaptic activity.

It was suggested previously that calpain activation contributes to long-term potentiation by proteolytic processing of cytoskeletal proteins, thereby changing the structure and efficacy of synapses (45). Our results indicate another potential role for calpains during long-term potentiation: the proteolytic processing and persistent regulation of postsynaptic class C L-type channels. NMDA application, which can cause long-term potentiation under certain circumstances (36), increases the activity of L-type channels in acutely exposed hippocampal pyramidal neurons (46), and strong activation of L-type Ca^{2+} channels can induce a sustained increase in synaptic efficacy that resembles long-term potentiation (47–49). Both NMDA-induced potentiation of synaptic transmission and proteolytic conversion of α_{1C} continue for at least 2–3 h (Fig. 2*A*; data not shown). Modification of α_{1C} may, therefore, contribute to the changes in neuronal function during the late phase of long-term potentiation by enhancing synaptic transmission, altering gene expression, or influencing restructuring of potentiated synapses, which is thought to be necessary for a permanent change of synaptic strength (50).

This work was supported by Faculty Scholar Award FSA-94-033 from the Alzheimer's Association (to J.W.H.), by the National Institutes of Health (to C.C. and W.A.C.), and by the W. M. Keck Foundation.

1. Walaas, S. I. & Greengard, P. (1991) *Pharmacol. Rev.* **43,** 299–349.
2. Ghosh, A. & Greenberg, M. E. (1995) *Science* **268,** 239–247.
3. Bear, M. F. & Malenka, R. C. (1994) *Curr. Opin. Neurobiol.* **4,** 389–399.
4. Dunlap, K., Luebke, J. I. & Turner, T. J. (1994) *Trends Neurosci.* **18,** 89–98.
5. Snutch, T. P. & Reiner, P. B. (1992) *Curr. Opin. Neurobiol.* **2,** 247–253.
6. Randall, A. & Tsien, R. W. (1995) *J. Neurosci.* **15,** 2995–3012.
7. Catterall, W. A. (1995) *Annu. Rev. Biochem.* **64,** 493–531.
8. Birnbaumer, L., Campbell, K. P., Catterall, W. A., Harpold, M. M., Hofmann, F., Horne, W. A., Mori, Y., Schwartz, A., Snutch, T. P., Tanabe, T. & Tsien, R. W. (1994) *Neuron* **13,** 505–506.
9. Snutch, T. P., Tomlinson, W. J., Leonard, J. P. & Gilbert, M. M. (1991) *Neuron* **7,** 45–57.
10. Williams, M. E., Feldman, D. H., McCue, A. F., Brenner, R., Velicelebi, G., Ellis, S. B. & Harpold, M. M. (1992) *Neuron* **8,** 71–84.
11. Hell, J. W., Westenbroek, R. E., Warner, C., Ahlijanian, M. K., Prystay, W., Gilbert, M. M., Snutch, T. P. & Catterall, W. A. (1993) *J. Cell Biol.* **123,** 949–962.
12. Lerea, L. S., Butler, L. S. & McNamara, J. O. (1992) *J. Neurosci.* **12,** 2973–2981.
13. Elliott, E. M., Malouf, A. T. & Catterall, W. A. (1995) *J. Neurosci.* **15,** 6433–6444.
14. Westenbroek, R. E., Ahlijanian, M. K. & Catterall, W. A. (1990) *Nature (London)* **347,** 281–284.
15. Ahlijanian, M. K., Westenbroek, R. E. & Catterall, W. A. (1991) *Neuron* **4,** 819–832.
16. De Jongh, K. S., Merrick, D. K. & Catterall, W. A. (1989) *Proc. Natl. Acad. Sci. USA* **86,** 8585–8589.
17. De Jongh, K. S., Warner, C., Colvin, A. A. & Catterall, W. A. (1991) *Proc. Natl. Acad. Sci. USA* **88,** 10778–10782.
18. Rotman, E. I., De Jongh, K. S., Florio, V., Lai, Y. & Catterall, W. A. (1992) *J. Biol. Chem.* **267,** 16100–16105.
19. Rotman, E. I., Murphy, B. J. & Catterall, W. A. (1995) *J. Biol. Chem.* **270,** 16371–16377.
20. Hell, J. W., Yokoyama, C. T., Wong, S. T., Warner, C., Snutch, T. P. & Catterall, W. A. (1993) *J. Biol. Chem.* **268,** 19451–19457.
21. Hell, J. W., Yokoyama, C. T., Breeze, L. J., Chavkin, C. & Catterall, W. A. (1995) *EMBO J.* **14,** 3036–3044.
22. Wei, X., Neely, A., Lacerda, A. E., Olcese, R., Stefani, E., Perez-Reyes, E. & Birnbaumer, L. (1994) *J. Biol. Chem.* **269,** 1635–1640.
23. Klöckner, U., Mikala, G., Varadi, M., Varadi, G. & Schwartz, A. (1995) *J. Biol. Chem.* **270,** 17306–17310.
24. Hollmann, M. & Heinemann, S. (1994) *Annu. Rev. Neurosci.* **17,** 31–108.
25. Wang, K. K. & Yuen, P. W. (1994) *Trends Pharmacol. Sci.* **15,** 412–419.
26. Kawashima, S., Nomoto, M., Hayashi, M., Inomata, M., Nakamura, M. & Imahori, K. (1984) *J. Biochem. (Tokyo)* **95,** 95–101.
27. Wang, K. K. W., Roufogalis, B. D. & Villalobo, A. (1988) *Arch. Biochem. Biophys.* **260,** 317–327.
28. Westenbroek, R. E., Hell, J. W., Warner, C., Dubel, S. J., Snutch, T. B. & Catterall, W. A. (1992) *Neuron* **9,** 1099–1115.
29. Dubel, S. J., Starr, T. V. B., Hell, J., Ahlijanian, M. K., Enyeart, J. J., Catterall, W. A. & Snutch, T. P. (1992) *Proc. Natl. Acad. Sci. USA* **89,** 5058–5062.
30. Yokoyama, C. T., Westenbroek, R. E., Hell, J. W., Soong, T. W., Snutch, T. P. & Catterall, W. A. (1995) *J. Neurosci.* **15,** 6419–6432.
31. Westenbroek, R. E., Westrum, L. E., Hendrickson, A. E. & Wu, J.-Y. (1988) *J. Comp. Neurol.* **274,** 334–346.
32. Wagner, J. J., Terman, G. W. & Chavkin, C. (1993) *Nature (London)* **363,** 451–454.
33. Petralia, R. S., Yokotani, N. & Wenthold, R. J. (1994) *J. Neurosci.* **14,** 667–696.
34. Yuste, R. & Denk, W. (1995) *Nature (London)* **375,** 682–684.
35. Segal, M. (1995) *J. Physiol. (London)* **486,** 283–295.
36. Malenka, R. C. (1991) *Neuron* **6,** 53–60.
37. Sculptoreanu, A., Rotman, E., Takahashi, M., Scheuer, T. & Catterall, W. A. (1993) *Proc. Natl. Acad. Sci. USA* **90,** 10135–10139.
38. Hell, J. W., Appleyard, S. M., Yokoyama, C. T., Warner, C. & Catterall, W. A. (1994) *J. Biol. Chem.* **269,** 7390–7396.
39. Niidome, T., Kim, M.-S., Friedrich, T. & Mori, Y. (1992) *FEBS Lett.* **308,** 7–13.
40. Foster, A. C. & Fagg, G. E. (1987) *Nature (London)* **329,** 395–396.
41. MacDermott, A. B., Mayer, M. L., Westbrook, G. L., Smith, S. J. & Barker, J. L. (1986) *Nature (London)* **321,** 519–522.
42. Moriyoshi, K., Masu, M., Ishii, T., Shigemoto, R., Mizuno, N. & Nakanishi, S. (1991) *Nature (London)* **354,** 31–38.
43. Perlmutter, L. S., Siman, R., Gall, C., Seubert, P., Baudry, M. & Lynch, G. (1988) *Synapse* **2,** 79–88.
44. Siman, R. & Noszek, J. K. (1988) *Neuron* **1,** 279–287.
45. Lynch, G. & Baudry, M. (1984) *Science* **224,** 1057–1063.
46. Chetkovich, D. M., Gray, R., Johnston, D. & Sweatt, J. D. (1991) *Proc. Natl. Acad. Sci. USA* **88,** 6467–6471.
47. Grover, L. M. & Teyler, T. J. (1990) *Nature (London)* **347,** 477–479.
48. Aniksztejn, L. & Ben-Ari, Y. (1991) *Nature (London)* **349,** 67–69.
49. Kullmann, D. M., Perkel, D. J., Manabe, T. & Nicoll, R. A. (1992) *Neuron* **9,** 1175–1183.
50. Bailey, C. H., Chen, M., Keller, F. & Kandel, E. R. (1992) *Science* **256,** 645–649.